

Feasible and cost-effective three-level temperature control circuit design for automotive industry seat heater system applications

Hakan TEKİN¹, Eren MURTULU¹

¹Seğer Ses ve Elektrikli Gereçler San. A.Ş. Bursa, Türkiye

Abstract - Seat heater is an electronic circuit-based topology designed for optimizing vehicle heating systems and enhancing passenger comfort in low-temperature weather conditions. To can implement a design in a real word automotive system, the necessary standards for this section should be considered. This study presents a step-by-step design of a three-level temperature control circuit seat heater system for automotive industry applications. the designed schematic of the switching circuit is presented and detailed code comments and explanations are provided for the micro controller unit (MCU) regarding occupancy sensor analysis, setting heater operation based on passenger selection, and controlling current loops for the seat heater circuit.

Key Words: Seat heater, Automotive industry, Micro controller, Three level temperature control, printed circuit board (PCB) design.

1. INTRODUCTION

Although the seat heater systems have been designed and used in automobiles since 1970, and according to 2010 U.S. automotive data, more than 30 percent of automobiles have been equipped with these systems, normally they don't follow any specific individual or mandatory industrial standards [1-2].

This causes some of these designs to not be used in an optimized way and to generate heat that is more than the sufferable temperature for passengers.

Some of the designs could not introduce automatic turn-off systems over time, which can generate serious heat problems for occupants who suffer lower body sensory deficits caused by paralysis, diabetes, and neuropathy [1].

For internal combustion engine cars, normally the power for elements like the wipers, lighting, heating, and cooling systems is supplied by the alternator, which normally charges the battery over time [3-4].

With the growing demand for electric vehicles (EVs), the application of fully electronics-based systems is increasing.

In these cars, the mentioned parts are supplied by the battery pack system [5-8].

Therefore, an optimized application of electric energy can be helpful for battery health and a longer lifespan. On the other

hand, normally different ranges of battery voltages are generated and used in the automotive industry. Therefore, designing a circuit that is capable of working in a wide range of input voltages and generating a fixed DC voltage is essential [9-10].

Another important parameter that can increase the longevity of the battery system is establishing a current with minimum ripple amplitude in the battery, even if there is a large difference between the battery pack and the target DC voltage for the mentioned circuits [11-13].

DC-DC converters have been analyzed in literature [14-19]. This type of converters is used in EVs for different parts like the lighting, cooling or heating, wiper system, sound circuits, etc.

A micro controller system should manage the generated power and power distribution for these parts. One of the optional parts is seat heater system that is essential for cold weathers.

In this study, a three level heating system for automotive industry is presented to generate 3A, 4A and 4.5A for the seats in a car based on the passenger request by pressing a button system The Attiny 1616 MCU is used in experimental tests, and all code comments regarding the analog-to-digital conversions, seat occupation check, and three-level heating button control to adjust the level of current in the heater system based on temperature and passenger comfort are presented.

2. HEAT CONTROL SYSTEM DESIGN STEPS

Figure 1 shows the circuit topology that switches the load. The integrated circuit shown as U2 is a coded-type power switch and corresponds to the BTS6143D product.

When a signal is applied to the switch's IN pin, it transfers the voltage from the VBB input pin to the OUT pin. The output current can be controlled by a PWM signal applied to the IN pin.

The switch features short-circuit protection, current limiting, over temperature detection, and load detection. Because the switch's R_{dsON} resistance is very low, it can conduct a continuous current. Furthermore, the switch can supply a load current of up to 8 A.

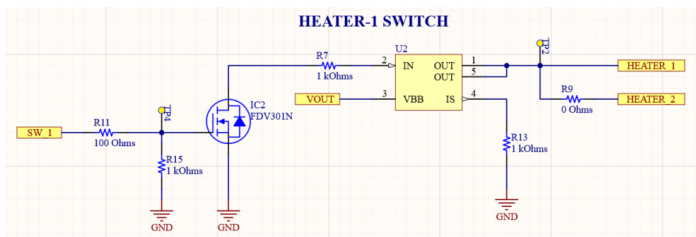


Figure 1. Schematic design of the switching circuit.

Figure 2 shows the schematic design of the MCU used in the circuit. The ATtiny1616 microcontroller from Microchip is used here. The MCU is powered by a 5 V regulator.

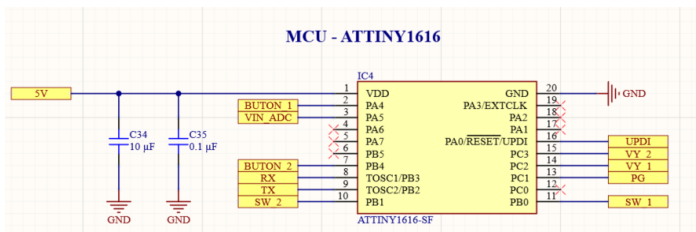


Figure 2. MCU schematic design.

This subsection presents the code comments for current sensor data reading and conversion from analog to digital format, as well as current adjustments for the heating pad based on the heat level selected by the passenger through a 3-level temperature adjustment button for each pad system. The general flowchart of the MCU is presented in figure 3 and shows the operational steps in detail.

For the first stage, the MCU reads the input voltage (battery voltage).

The system operates if the battery voltage is within the desired range (9–32 V); otherwise, it does not operate. This is done using the voltage information obtained from the voltage divider shown below.

The related code comments have been presented in Figures 4a and 4b under titles: `adc_calculation.c/adc_calculation.h`

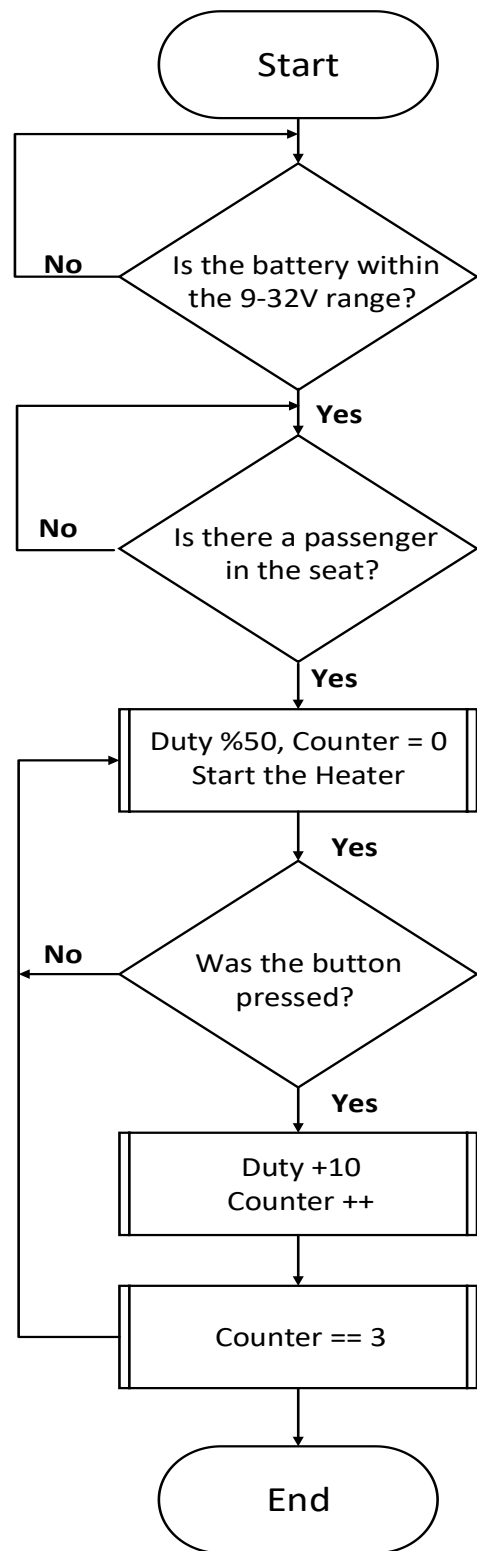


Figure 3. MCU operation flowchart.

```
#include <avr/io.h>
#include "adc_calculation.h"

/* RTC Period */
#define RTC_PERIOD      (511)

void ADC0_init(void)
{
    /* Disable digital input buffer */
    PORTA.PINSCTRL &= ~PORT_ISC_bm;
    PORTA.PINSCTRL |= PORT_ISC_INPUT_DISABLE_gc;

    /* Disable pull-up resistor */ PORTA.PINSCTRL &= ~PORT_PULLUPEN_bm;

    ADC0.CTRLB = ADC_PRESC_DIV4_gc /* CLK_PER divided by 4 */
    | ADC_REFSEL_VDDREF_gc; /* External reference */

    ADC0.CTRLA = ADC_ENABLE_bm /* ADC Enable: enabled */
    | ADC_RESSEL_10BIT_gc; /* 10-bit mode */

    /* Select ADC channel */
    ADC0.MUXPOS = ADC_MUXPOS_AINS5_gc;
}

uint16_t ADC0_read(void)
{
    /* Start ADC conversion */
    ADC0.COMMAND = ADC_STCONV_bm;

    /* Wait until ADC conversion done */
    while ( !(ADC0.INTFLAGS & ADC_RESRDY_bm) )
    {
        ;
    }

    /* Clear the interrupt flag by writing 1: */
    ADC0.INTFLAGS = ADC_RESRDY_bm;

    return ADC0.RES;
}
```

(a)

```
#include "ocupancy_reading.h"
volatile uint8_t but3, but4;

void OCUPANCY_init(void) {
    PORTC.DIR &= ~(PIN2_bm | PIN3_bm);
    PORTC.PIN2CTRL |= PORT_PULLUPEN_bm | PORT_ISC_BOTHEDGES_gc;
    PORTC.PIN3CTRL |= PORT_PULLUPEN_bm | PORT_ISC_BOTHEDGES_gc;

    sei();
}

ISR(PORTC_PORT_vect) {
    if (PORTC.INTFLAGS & PIN2_bm) {
        if (PORTC.IN & PIN2_bm) {
            but3 = 1; // PC2 HIGH
        } else {
            but3 = 0; // PC2 LOW
        }
        PORTC.INTFLAGS = PIN2_bm;
    }

    if (PORTC.INTFLAGS & PIN3_bm) {
        if (PORTC.IN & PIN3_bm) {
            but4 = 1; // PC3 HIGH
        } else {
            but4 = 0; // PC3 LOW
        }
        PORTC.INTFLAGS = PIN3_bm;
    }
}
```

(a)

```
#ifndef ADC_CALCULATION_H_
#define ADC_CALCULATION_H_

#include <stdint.h>

#define ADC_REF_VOLTAGE      5.0
#define ADC_RESOLUTION      1023.0

#define BATTERY_VOLTAGE_MIN 0.750
#define BATTERY_VOLTAGE_MAX 2.420

uint16_t adcVal;

void ADC0_init(void);
uint16_t ADC0_read(void);

#endif /* ADC_CALCULATION_H_ */
```

(b)

Figure 4. (a) adc_calculation.c and (b) adc_calculation.h code comments

The next stage of the process checks whether a seat is occupied via the presence/absence by checking the data of the seat occupancy sensor. If a passenger is seated, the system operates, providing the heating function. If no one is seated, the system remains inactive. The code comments for this stage have been presented in Figures 5a and 5b with titles: **ocupancy_reading.c / ocupancy_reading.h**

```
#ifndef OCUPANCY_READING_H_
#define OCUPANCY_READING_H_

#include <avr/io.h>
#include <avr/interrupt.h>

extern volatile uint8_t but3, but4;

void OCUPANCY_init(void);

#endif /* OCUPANCY_READING_H_ */
```

(b)

Figure 5. (a) ocupancy_reading.c and (b) ocupancy_reading.h code comments

When a passenger is seated, the user can adjust the temperature in three stages using a button. The temperature is adjusted by controlling the current flow through the load. The first stage is controlled by the switch at a 50% duty cycle generating 3A current in pad system, the second at a 60% duty cycle with presenting 4 A, and the third at a 70% duty cycle by generating 4.5 A for seat pad system. The code comments for his operational modes figures 6a and 6b are presented with general title of **buton_readin.c / buton_reading.h**:

```
#include "button_reading.h"
volatile uint8_t but1, but2;

void BUTTONS_init(void) {
    PORTA.DIR &= ~PIN4_bm;
    PORTA.PIN4CTRL |= PORT_PULLUPEN_bm | PORT_ISC_BOTHEDGES_gc;

    PORTB.DIR &= ~PIN4_bm;
    PORTB.PIN4CTRL |= PORT_PULLUPEN_bm | PORT_ISC_BOTHEDGES_gc;

    sei();
}

ISR(PORTA_PORT_vect) {
    if (PORTA.INTFLAGS & PIN4_bm) {
        if (PORTA.IN & PIN4_bm) {
            but1 = 1; // PA4 HIGH
        } else {
            but1 = 0; // PA4 LOW
        }
        PORTA.INTFLAGS = PIN4_bm;
    }
}

ISR(PORTB_PORT_vect) {
    if (PORTB.INTFLAGS & PIN4_bm) {
        if (PORTB.IN & PIN4_bm) {
            but2 = 1; // PB4 HIGH
        } else {
            but2 = 0; // PB4 LOW
        }
        PORTB.INTFLAGS = PIN4_bm;
    }
}
```

(a)

```
#ifndef BUTTON_READING_H_
#define BUTTON_READING_H_

#include <avr/io.h>
#include <avr/interrupt.h>

extern volatile uint8_t but1, but2;

void BUTTONS_init(void);

#endif /* BUTTON_READING_H_ */
```

(b)

```
#include "switch_pwm.h"

void TCA0_init(void)
{
#ifdef PORTMUX_TCA0_PORTB_gc
    PORTMUX.TCA0ROUTEA = PORTMUX_TCA0_PORTB_gc;
#endif

    TCA0.SINGLE.CTRLB = TCA_SINGLE_CMP0EN_bm
        | TCA_SINGLE_CMP1EN_bm
        | TCA_SINGLE_WGMODE_DSBOTTOM_gc;

    TCA0.SINGLE.EVCTRL &= ~(TCA_SINGLE_CNTEI_bm);

    TCA0.SINGLE.PER = F_CPU / PWM_FREQUENCY - 1;
    TCA0.SINGLE.CMP0BUF = (TCA0.SINGLE.PER * 50) / 100;
    TCA0.SINGLE.CMP1BUF = (TCA0.SINGLE.PER * 50) / 100;

    TCA0.SINGLE.CTRLA = TCA_SINGLE_CLKSEL_DIV4_gc
        | TCA_SINGLE_ENABLE_bm;
}

void PORT_init(void)
{
    PORTB.DIR |= PIN0_bm | PIN1_bm;
}
```

(a)

```
#ifndef SWITCH_PWM_H_
#define SWITCH_PWM_H_

#include <avr/io.h>

#define F_CPU 16000000UL // 16 MHz

#define PWM_FREQUENCY 50000

void TCA0_init(void);
void PORT_init(void);

#endif /* SWITCH_PWM_H_ */
```

(b)

Figure 6. (a) buton_readin.c and (b) buton_reading.h code comments

Figure 7. (a) switch_pwm.c and (b) switch_pwm.h code comments

This section of the code makes the necessary adjustments to generate the PWM signal used to control the current flow of the heating pad. The relevant code commands are shown in Figures 7a and 7b, as well as in the general **switch_pwm.c** / **switch_pwm.h** headers.

The main.c code in Figure 8 contains the functions necessary for the overall operation of the system. If the system operates between 9–32 V and a passenger is seated, the system begins heating at a 50% duty cycle, corresponding to Stage 1. The user can adjust the setting using a button. After three settings, pressing the button again returns the system to Stage 1. If the seated passenger leaves, the heating process stops.

```
int main(void)
{
    system_init();

    while (1)
    {
        int adcVal = ADC0_read();

        batteryVoltage = ((adcVal * ADC_REF_VOLTAGE) / ADC_RESOLUTION);

        if (batteryVoltage >= BATTERY_VOLTAGE_MIN && batteryVoltage <= BATTERY_VOLTAGE_MAX)
        {
            if (but1 == 0)
            {
                TCA0.SINGLE.CMP0BUF = 0;
                TCA0.SINGLE.CMP1BUF = 0;
                continue;
            }

            if (but3 == 1 && previous_but3_state == 0)
            {
                _delay_ms(50);
                if (but3 == 1)
                {
                    but3_press_count++;

                    if (but3_press_count > 3)
                    {
                        but3_press_count = 1;
                    }
                }
            }
        }
    }
}
```

```

if (but3_press_count == 1)
{
    TCA0.SINGLE.CMP0BUF = ((uint32_t)TCA0.SINGLE.PER * 50) / 100;
    TCA0.SINGLE.CMP1BUF = ((uint32_t)TCA0.SINGLE.PER * 50) / 100;
}
else if (but3_press_count == 2)
{
    TCA0.SINGLE.CMP0BUF = ((uint32_t)TCA0.SINGLE.PER * 60) / 100;
    TCA0.SINGLE.CMP1BUF = ((uint32_t)TCA0.SINGLE.PER * 60) / 100;
}
else if (but3_press_count == 3)
{
    TCA0.SINGLE.CMP0BUF = ((uint32_t)TCA0.SINGLE.PER * 70) / 100;
    TCA0.SINGLE.CMP1BUF = ((uint32_t)TCA0.SINGLE.PER * 70) / 100;
}
previous_but3_state = but3;
}
else
{
    TCA0.SINGLE.CMP0BUF = 0;
    TCA0.SINGLE.CMP1BUF = 0;
}
}
return 0;
}
    
```

Figure 8. main.c code comments

3. TEST RESULTS

Figure 9a shows a three dimensions (3D) view of the seat control unit's printed circuit board (PCB).

The PCB is designed with four 1 oz copper layers, including the top and bottom layers serve as signal layers, layer 2 as ground, and layer 3 as power.

Oz presents a unit for weight of copper per square foot of PCB area.

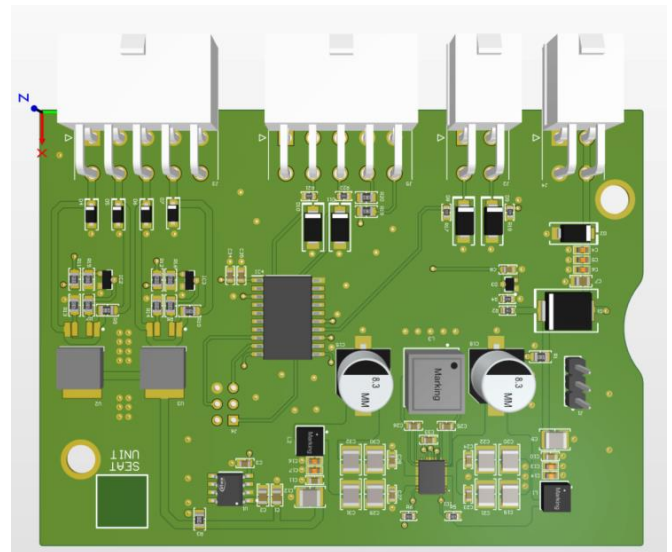
The integration of the design with the test setup in a laboratory environment is shown in Figure 9b.

The designed PCB was tested under three different input DC voltages that simulate the battery voltages. Since a buck-boost type power converter is tested in the prototype circuit, both lower and higher voltages than the desired 24 V DC output are considered.

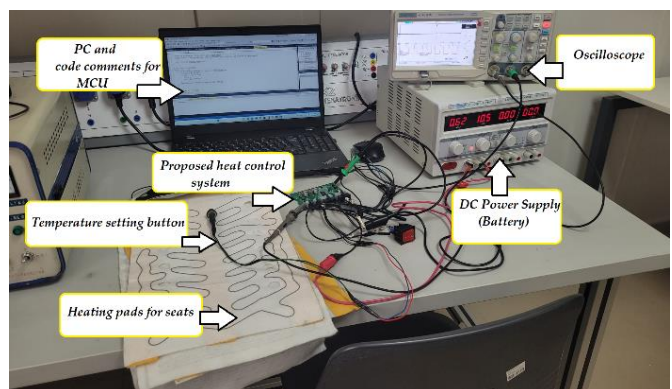
The tested input DC voltages are 10 V DC, 16 V DC, and 28 V DC, and the performance of the converter in stabilizing at 24 V DC are evaluated.

Figure 10a presents the output voltage of the PCB under 10 V input. Channel 1 shows the input voltage, and Channel 2 demonstrates the generated voltage of the proposed DC-DC converter.

As can be seen, although there is a large difference between the input and output voltages, the proposed circuit successfully generates an undamped 24 V DC output voltage.



(a)



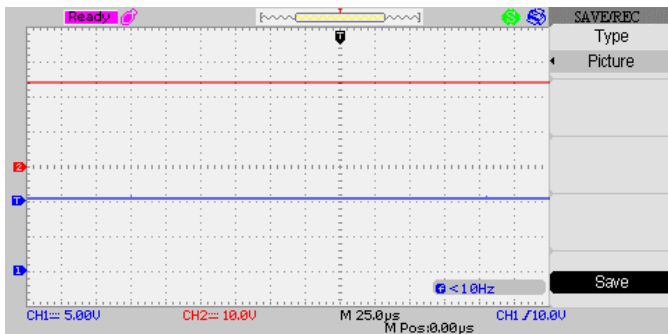
(b)

Figure 9. (a) 3D PCB view of the seat control unit, (b) laboratory work-bench.

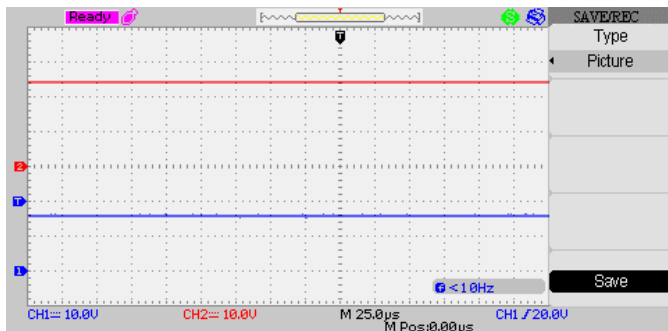
Figures 10b and 10c show the output voltage of the DC-DC converter for 16 V DC and 28 V DC input battery voltages.

As these results show, the quality of the converter output voltage remains unchanged, and an undamped, fixed 24 V DC is generated.

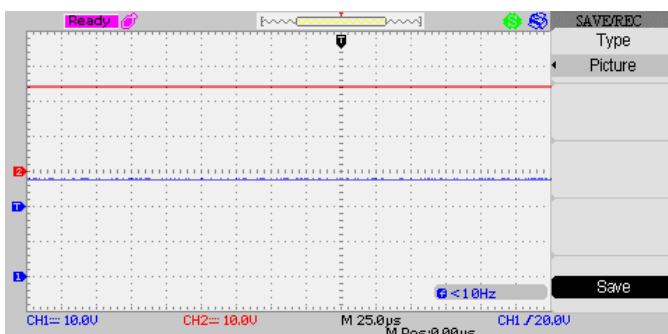
These results show that the design PCB can present a fixed DC voltage for a wide band of input voltage ranges that can be evaluated as an advantages for application in different automobiles with different battery DC voltages like the 12V or 24V without any need to set any parameter in the circuit. The test results show the capability of the topology for presenting a DC voltage that supplies the seat heater system. Presenting a variable DC voltage for heater can cause serious problems like the unstable current for the heater and low efficiency.



(a)



(b)



(c)

Figure 10. Generated a fixed 24 VDC output voltage for (a) 10VDC, (b) 16VDC and (c) 28VDC as the input battery DC voltages.

4. CONCLUSIONS

A new and practical seat heater circuit is presented in this study. All code comments regarding input battery limitation band checks, voltage polarity checks, and any short circuits in the system, along with the occupation sensor data and current control for the heating pads according to passenger selection, are presented thoroughly and in detail.

Laboratory test results are presented for fixing the DC voltage by the used converter to show how it can present a constant 24VDC for different input voltages from 10 to 30 VDC. The product was developed in the R&D section of Seger

A.Ş in Türkiye according to requests from automotive companies and is actively in use.

ACKNOWLEDGEMENT

This research was conducted in the R&D department of Seger Ses ve Elektrikli Gereçler San. A.Ş., Bursa, Türkiye, within the framework of industry–university cooperation with Bursa Technical University under the supervision of Dr. Ertekin. The authors thank the supervisor and his organization for their technical support.

REFERENCES

- [1] Safety Research & Strategies, Inc. 340 Anawan Street / Suite 200, Rehoboth, MA 02769, 2011.
- [2] D. Mihai, "Fuzzy control for temperature of the driver seat in a car," 2012 International Conference on Applied and Theoretical Electricity (ICATE), Craiova, Romania, 2012, pp. 1-8, doi: 10.1109/ICATE.2012.6403436.
- [3] A. Rajeev VK and V. Prasad, "Online Adaptive Gain for Passivity-Based Control for Sensorless BLDC Motor Coupled With DC Motor for EV Application," in IEEE Transactions on Power Electronics, vol. 38, no. 11, pp. 13625-13634, Nov. 2023, doi: 10.1109/TPEL.2023.3288939.
- [4] S. Mishra, A. Varshney, B. Singh and H. Parveen, "Driving-Cycle-Based Modeling and Control of Solar-Battery-Fed Reluctance Synchronous Motor Drive for Light Electric Vehicle With Energy Regeneration," in IEEE Transactions on Industry Applications, vol. 58, no. 5, pp. 6666-6675, Sept.-Oct. 2022, doi: 10.1109/TIA.2022.3181224.
- [5] Ertekin, D. ARVIN converter: a bidirectional DC/DC converter for grid-connected G2V/V2G energy storage and electrification approaches. *Electr Eng* 106, 5485–5505 (2024). <https://doi.org/10.1007/s00202-024-02295-x>
- [6] Huang R, Hong F, Ghaderi D. Sliding mode controller-based e-bike charging station for photovoltaic applications. *Int Trans Electr Energy Syst.* 2020;30:e12300. <https://doi.org/10.1002/2050-7038.12300>
- [7] T. Yuvaraj, K. R. Devabalaji, J. A. Kumar, S. B. Thanikanti and N. I. Nwulu, "A Comprehensive Review and Analysis of the Allocation of Electric Vehicle Charging Stations in Distribution Networks," in IEEE Access, vol. 12, pp. 5404-5461, 2024, doi: 10.1109/ACCESS.2023.3349274.
- [8] M. Asna, H. Shareef, A. Prasanthi, R. Errouissi and A. Wahyudie, "A Novel Multi-Level Charging Strategy for Electric Vehicles to Enhance Customer Charging

- Experience and Station Utilization," in IEEE Transactions on Intelligent Transportation Systems, vol. 25, no. 9, pp. 11497-11508, Sept. 2024, doi: 10.1109/TITS.2024.3372183.
- [9] Y. Xie, C. Wang, X. Hu, X. Lin, Y. Zhang and W. Li, "An MPC-Based Control Strategy for Electric Vehicle Battery Cooling Considering Energy Saving and Battery Lifespan," in IEEE Transactions on Vehicular Technology, vol. 69, no. 12, pp. 14657-14673, Dec. 2020, doi: 10.1109/TVT.2020.3032989.
- [10] K. Maalej, S. Kelouwani, K. Agbossou, Y. Dubé and N. Henao, "Long-Trip Optimal Energy Planning With Online Mass Estimation for Battery Electric Vehicles," in IEEE Transactions on Vehicular Technology, vol. 64, no. 11, pp. 4929-4941, Nov. 2015, doi: 10.1109/TVT.2014.2376700.
- [11] M. Özden, D. Ertekin and P. Siano, "Levenberg-Marquardt Algorithm-Based Neural Network Smart Control Strategy for a Low-Input Current Ripple and High-Voltage Gain Power Converter in Fuel-Cells Energy Systems," in IEEE Access, vol. 13, pp. 3613-3631, 2025, doi: 10.1109/ACCESS.2024.3524378.
- [12] Davut Ertekin, Mustafa Özden, Adnan Deniz, Muhammed Zeyd Toprak, Neuro-fuzzy-SVPWM switched-inductor-capacitor-based boost inverter for grid-tied fuel cell power generators, design and implementation, Renewable Energy, Volume 227, 2024, 120469, ISSN 0960-1481, <https://doi.org/10.1016/j.renene.2024.120469>.
- [13] Tekin, H. Setrekli, G. Murtumu, E.; Karşıyaka, H.; Ertekin, D. A Proposed Single-Input Multi-Output Battery-Connected DC-DC Buck-Boost Converter for Automotive Applications. Electronics 2023, 12, 4381. <https://doi.org/10.3390/electronics12204381>
- [14] H. Gholizadeh, M. Dehghan, R. S. Shahrivar, M. H. Samimi and M. Ghassemi, "A Non-Isolated Quadratic DC-DC Converter Improved by Voltage-Lift Technique Suitable for High-Voltage Applications," in IEEE Access, vol. 12, pp. 158292-158310, 2024, doi: 10.1109/ACCESS.2024.3484667.
- [15] M. Diwakar Naik, U. Vinatha, M. Venkatesh Naik and P. K. Bonthagorla, "Investigation and Performance Evaluation of Novel Single-Switch High-Gain DC-DC Converters for DC Microgrid Applications," in IEEE Access, vol. 13, pp. 103798-103808, 2025, doi: 10.1109/ACCESS.2025.3579261.
- [16] K. -M. Kim, "High-Efficiency Resonant DC-DC Converter With Low Input Current Ripple for DC Power Distribution Systems," in IEEE Access, vol. 12, pp. 85983-85994, 2024, doi:10.1109/ACCESS.2024.3416614.
- [17] Ghaderi, D.; Maroti, P.K.; Sanjeevikumar, P.; Holm-Nielsen, J.B.; Hossain, E.; Nayyar, A. A Modified Step-Up Converter with Small Signal Analysis-Based Controller for Renewable Resource Applications. Appl.Sci. 2020, 10, 102. <https://doi.org/10.3390/app10010102>
- [18] Efficiency Improvement for a DC-DC Quadratic Power Boost Converter by Applying a Switch Turn-off Lossless Snubber Structure Based on Zero Voltage Switching. (2018). Elektronika Ir Elektrotechnika, 24(3), 15-22. <https://doi.org/10.5755/j01.eie.24.3.20977>
- [19] Ertekin, D.; Baltacı, K.; Çelebi, M. Advancing Renewable Energy: An Experimental Study of a Switched-Inductor, Switched-Capacitor Luo Boost Converter for Low-Voltage Applications. Electronics 2023, 12, 5006. <https://doi.org/10.3390/electronics12245006>

BIOGRAPHIES

Hakan Tekin received his Bachelor's degree from Firat University in 2021 and his Master's degree from Bursa Technical University in 2023. He is currently pursuing his doctoral studies at Bursa Technical University. He is currently working as an embedded systems design engineer at Seger Ses ve Elektrikli Gereçler San. A.S. His research and areas of interest include power electronics, DC-DC converters, control circuits, electric vehicles, and acoustic device designs.

Eren Murtulu received his Bachelor's degree from İskenderun Technical University in 2021. He is currently working as an electronics project engineer at Seger Ses ve Elektrikli Gereçler San. A.Ş., where he is responsible for managing electronic project processes, creating system designs, and defining design inputs. His professional interests include electronic system design, embedded systems, and process management in automotive electronics.